Stem Cell Reports, Volume *16*

Supplemental Information

Astrocytic reactivity triggered by defective autophagy and metabolic failure causes neurotoxicity in frontotemporal dementia type 3

Abinaya Chandrasekaran, Katarina Stoklund Dittlau, Giulia I. Corsi, Henriette Haukedal, Nadezhda T. Doncheva, Sarayu Ramakrishna, Sheetal Ambardar, Claudia Salcedo, Sissel I. Schmidt, Yu Zhang, Susanna Cirera, Maria Pihl, Benjamin Schmid, Troels Tolstrup Nielsen, Jørgen E. Nielsen, Miriam Kolko, Julianna Kobolák, András Dinnyés, Poul Hyttel, Dasaradhi Palakodeti, Jan Gorodkin, Ravi S. Muddashetty, Morten Meyer, Blanca I. Aldana, and Kristine K. Freude

Supplemental Information

Supplemental table of contents

Figure S1. Transcriptome analysis. Related to Figure 3-5.
Figure S2. Characterization of autophagy at different rapamycin treatment concentrations. Related to Figure 2.
Figure S3. Characterization of autophagy changes with 500 nM rapamycin treatment. Related to Figure 2.
Figure S4. Characterization of mitophagy and TEM ultrastructural analysis. Related to Figure 2-3.
Figure S5. Metabolic Response to Glutamate/Glucose and Cytokine Profile. Related to Figure 4-5.

Table S1. Overview of cell lines. Related to Figure 1.
Table S2. Selected differentially expressed genes. Related to Figure 3-5.
Table S3. Differentially expressed genes. Related to Figure 3-5.
Table S4. Antibodies used for Immunocytochemistry, Western blot and Primers used for RT-qPCR. Related to Figure 1-3 and 5.

Supplemental Experimental Procedures

Supplemental References

Supplemental Figures

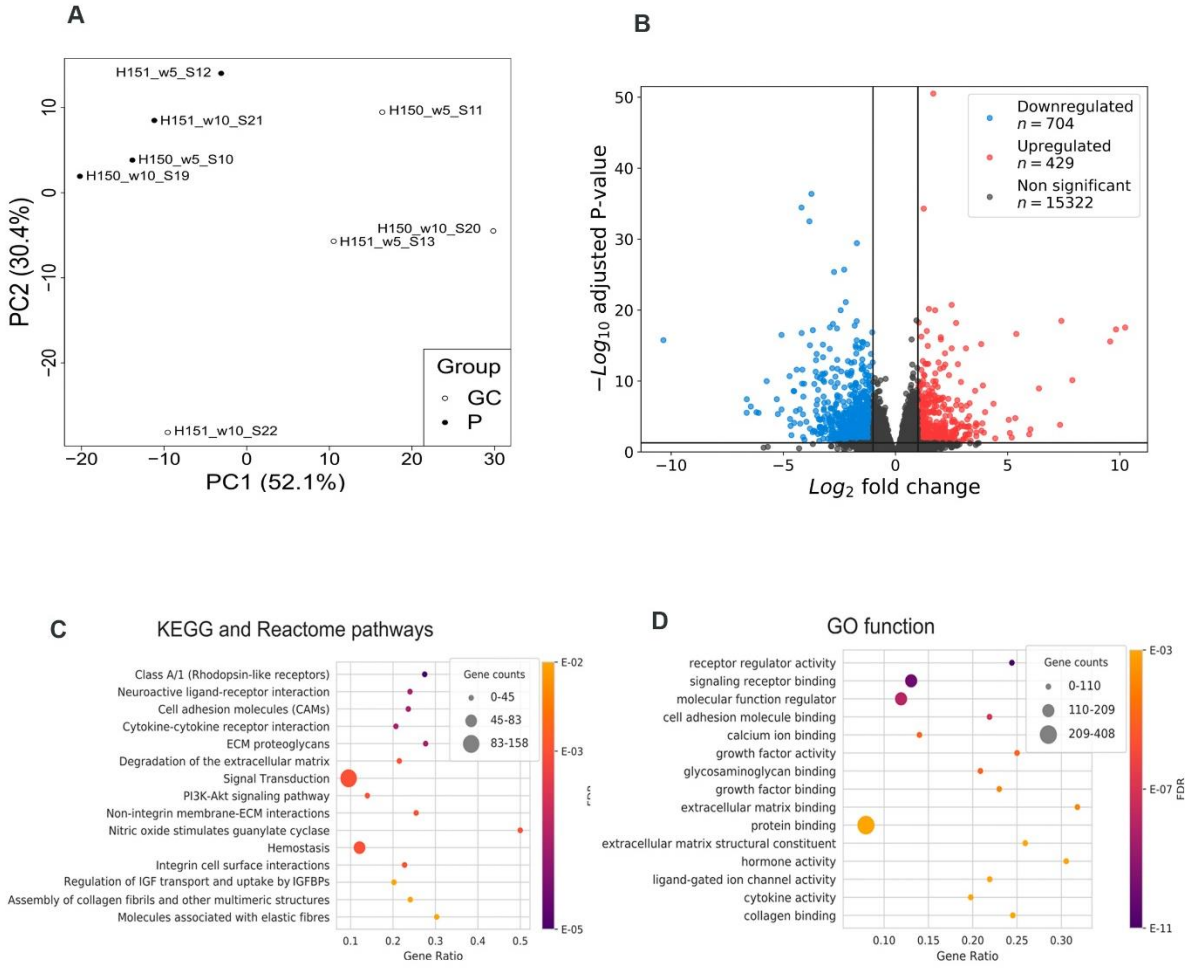

Figure S1. Transcriptome analysis. Related to Figure 3-5.
Expression-based Principal Component (PC) analysis shows consistent separation between FTD3 patient astrocytes and isogenic controls. The results consistently separated FTD3 patient lines and control lines based on their gene expression levels via PC analysis. **B)** Volcano plot of genes with a mean of DESeq2-normalized counts >= 10 differentially expressed between FTD3 patient astrocytes and isogenic controls. Genes with absolute log2FoldChange >= 1 and adjusted p-value <= 0.05 are selected as significantly differentially expressed and colored in blue or red if down- or upregulated, respectively. Analysis of differential gene expression between patient and control astrocytes, revealed 1,133 genes with a log2 fold change (LFC) of gene expression ≥ 1; and a significant P-value (<=0.05) after adjusting for multiple testing **C)** Top 15 significantly enriched KEGG and Reactome pathways identified by functional enrichment analysis of all 1133 significantly differentially expressed genes between FTD3 patient astrocytes and isogenic controls. The gene ratio corresponds to the ratio between the differentially expressed and all expressed genes annotated with a term. For each enriched term, the size of the dot indicates the number of differentially expressed genes annotated with this term, while the color shows the FDR of the enrichment test. **D**) The same representation as in (c) is used for the top 15 significantly enriched Gene Ontology (GO) functions.

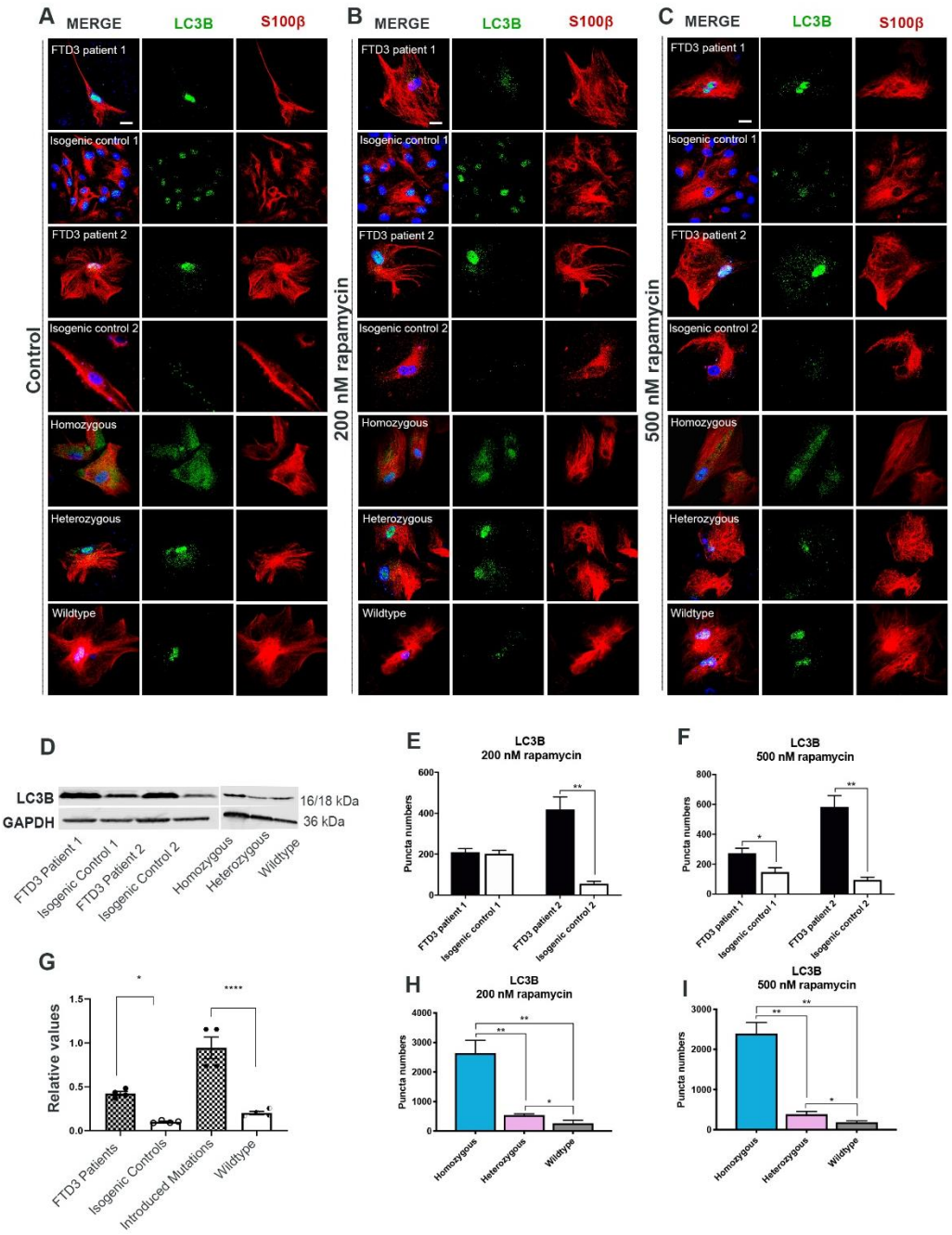

Figure S2. Characterization of autophagy at different rapamycin treatment concentrations. Related to Figure 2.

A-C) Representative ICC images of LC3B and S100β co-labelling of astrocytes at 0nM, 200nM and 500nM rapamycin treatment. LC3B is a marker of autophagosomes. S100B is utilized as a cytoplasmic marker to visualize LC3B intracellular distribution. Scale bar, 25 µm. **D+G)** WB analysis of LC3B. Data represented as mean ± SEM. One-way ANOVA with Tukey multiple comparisons test; *p<0.05 and ****p <0.0001. **E-F+H-I)** LC3B puncta number quantification of astrocytes at different rapamycin concentrations. Data represented as mean ± SEM of three independent experiments. One-way ANOVA with Tukey multiple comparisons test; *p<0.05 and **p <0.01.

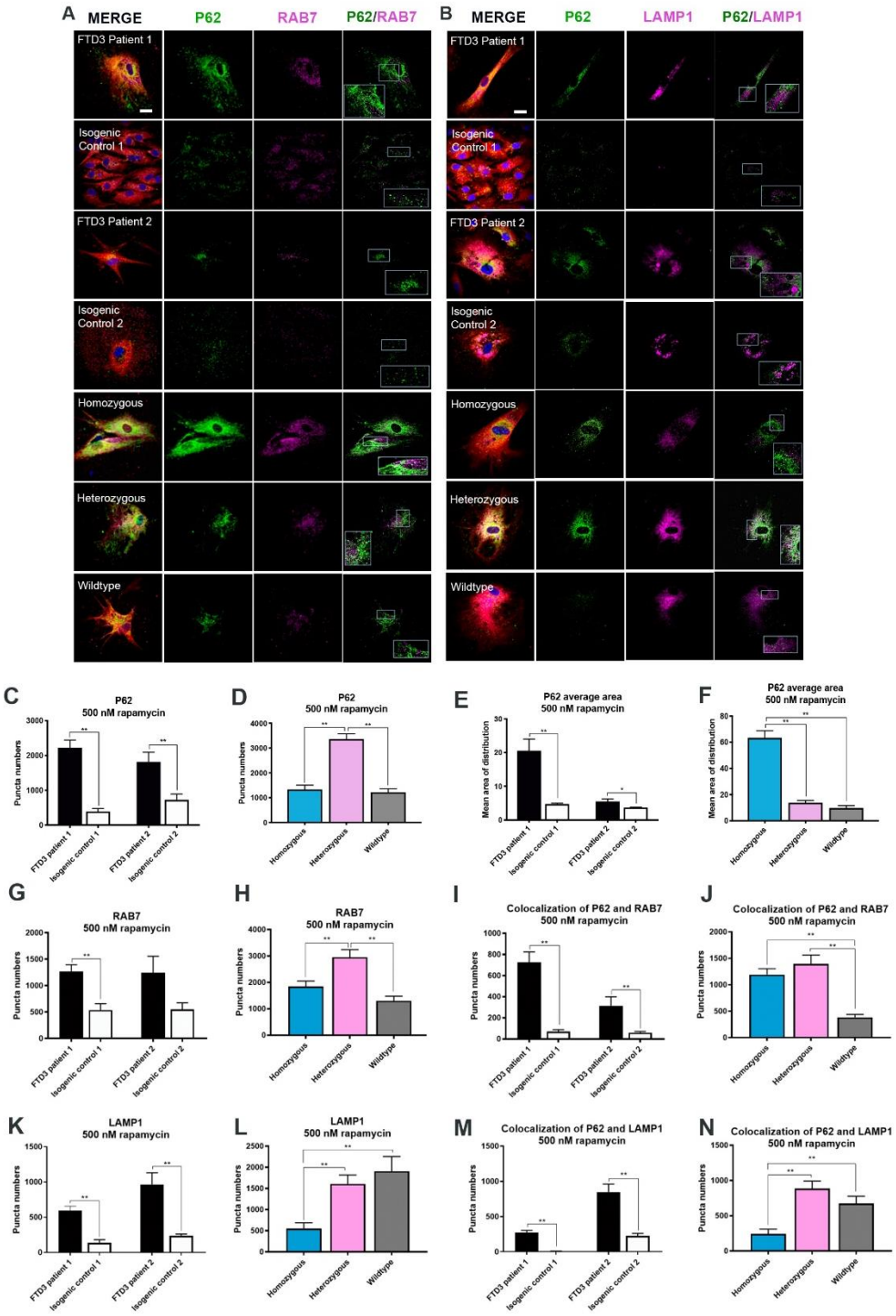

Figure S3. Characterization of autophagy changes with 500 nM rapamycin treatment. **Related to Figure 2.**

A-B) Representative ICC images of P62, AQP4 and RAB7 (**A**) and P62, AQP4 and LAMP1 (**B**) co-labelling of astrocytes with 500 nM rapamycin treatment. Scale bar, 25 µm. **C-J)** ICC quantifications of P62, RAB7, and P62 mean area and co-localization puncta number of FTD3 patient, heterozygous, homozygous astrocytes vs controls. Data represented as mean ± SEM of three independent experiments. One-way ANOVA with Tukey multiple comparisons test; *p<0.05 and **p <0.01. **K-N)** LAMP1 and co-localization puncta number quantification of FTD3 astrocytes and controls with 500 nM rapamycin treatment. Data

represented as mean ± SEM. One-way ANOVA with Tukey multiple comparisons test; *p<0.05, **p <0.01 and ***p <0.001.

Figure S4

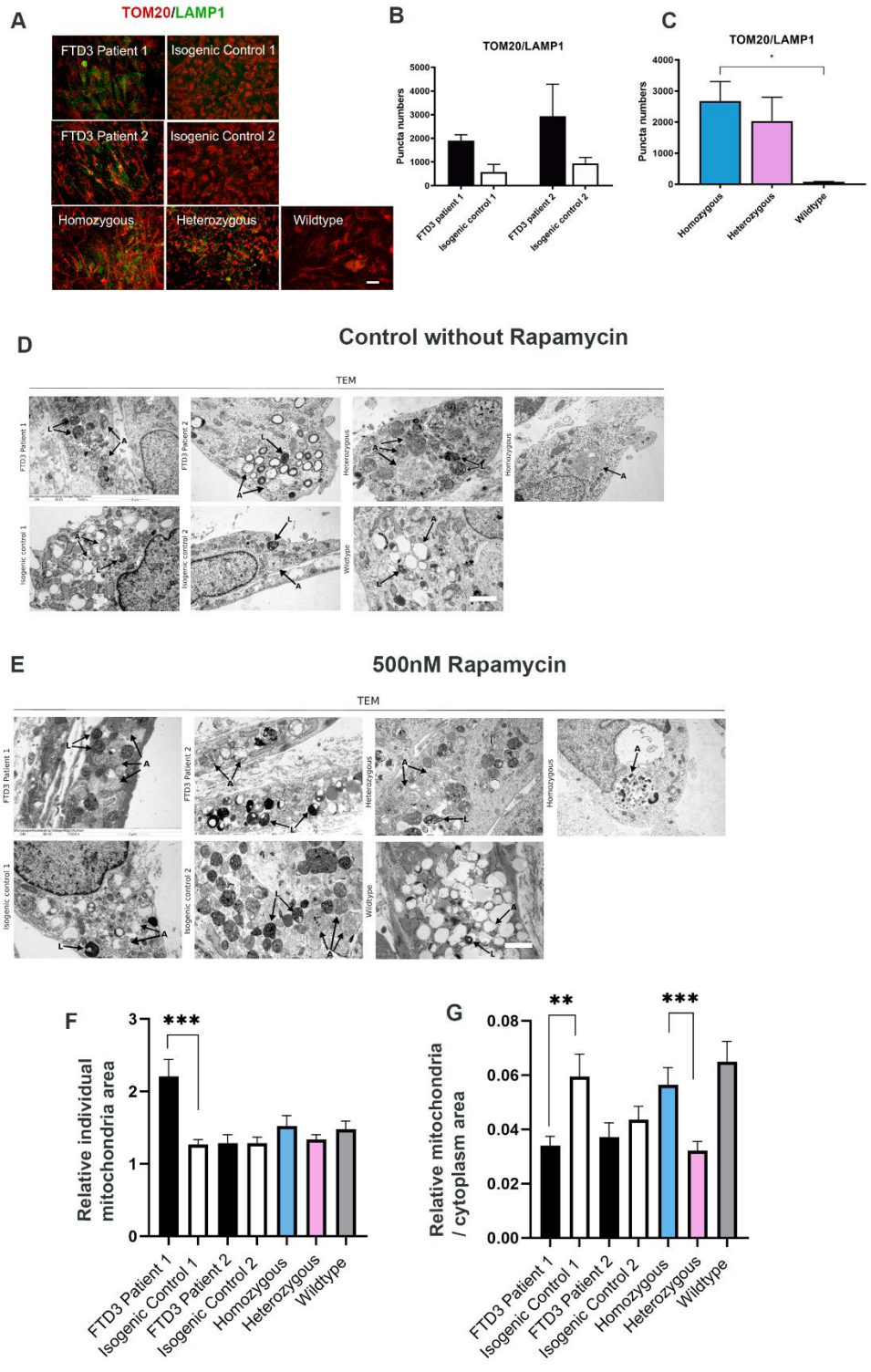
A
TOM20/LAMP1
FTD3 Patient 1
Isogenic Control 1
FTD3 Patient 2
Isogenic Control 2
Homozygous
Heterozygous
Wildtype
B
TOM20/LAMP1
Puncta numbers
FTD3 patient 1
Isogenic control 1
FTD3 patient 2
Isogenic control 2
C
TOM20/LAMP1
Puncta numbers
Homozygous
Heterozygous
Wildtype
D
Control without Rapamycin
TEM
E
500nM Rapamycin
TEM
F
Relative individual mitochondria area
FTD3 Patient 1
Isogenic Control 1
FTD3 Patient 2
Isogenic Control 2
Homozygous
Heterozygous
Wildtype
G
Relative mitochondria / cytoplasm area
FTD3 Patient 1
Isogenic Control 1
FTD3 Patient 2
Isogenic Control 2
Homozygous
Heterozygous
Wildtype

Figure S4. Characterization of mitophagy and TEM ultrastructural analysis. Related to Figure 2-3. **A)** Representative ICC images of TOM20 and LAMP1 co-labelling. Scale bar, 25 µm. **B-C**) Quantifications of TOM20 and LAMP1 co-localization. Data represented in mean ± SEM. One-way ANOVA with Tukey multiple comparisons test; *p<0.05. **D-E)** Representative TEM images of astrocytes at 10 weeks of maturation. FTD3 astrocyte lines demonstrate an increase in electron-dense cargo-filled vesicles. Control without rapamycin treatment (**D**). 500nM rapamycin treatment **(E**). Examples of autophagosomes and autolysosomes are indicated with black arrows. (A= autophagosomes and L= autolysosomes), Scale bar=2µm. **F)** TEM quantitative analysis of relative individual mitochondria area. Data represented in mean ± SEM of three independent experiments. Unpaired t-test with Welch's. Significance differences are indicated with ***p < 0.001. **G)** TEM quantitative analysis of relative mitochondria to cytoplasm area ratio. Data represented as mean ± SEM. Unpaired t-test with Welch's. Significance differences are indicated with **p < 0.01, ***p < 0.001.

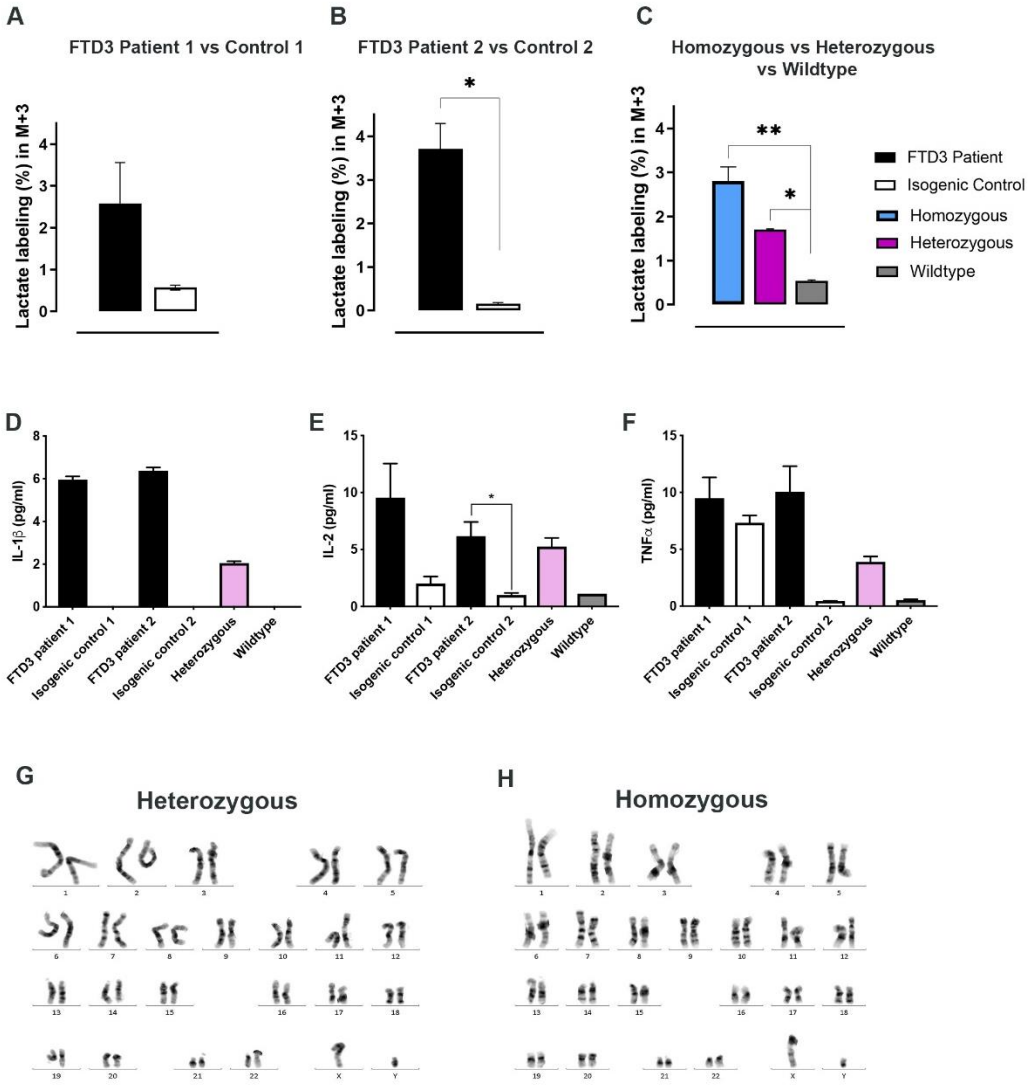

Figure S5. Metabolic Response to Glutamate/Glucose and Cytokine Profile. Related to Figure 4-5. A-C) Labeling percentage in lactate M + 3 in hIPSC-derived astrocytes after incubation with [U-^{13}C]glutamate and unlabeled glucose. **D-F)** Cytokine Profiling of IL-2, TNF α and IL-1β) of FTD3 related astrocyte lines compared to its controls. Data represented in mean ± SEM of three independent experiments. One-way ANOVA with Tukey multiple comparisons test; *p<0.05. **G-H)** Karyogram of heterozygous induced CHMP2B mutation (left) and homozygous induced CHMP2B mutation (right). Both cell lines expressed normal karyotype profile.

Supplemental Tables

Table S1. Overview of cell lines. Related to Figure 1.

hiPSC Line	Genotype	Karyotype	Pluripotency-associated Marker	Gender	References
H150 (FTD3 patient 1)	G/C 31449 in CHMP2B	Normal	+	M	Yu Zhang et al 2017
H151 (FTD3 patient 2)	G/C 31449 in CHMP2B	Normal	+	M	Yu Zhang et al 2017
H150 ISO (Isogenic control 1)	Gene corrected	Normal	+	M	Yu Zhang et al 2017
H151 ISO (Isogenic control 2)	Gene corrected	Normal	+	M	Yu Zhang et al 2017
K3 p53++	Homozygous mutant	Normal	+	M	Added to Figure S5
K3 p53+-	Heterozygous mutant	Normal	+	M	Added to Figure S5
K3 p53	Wild type	Normal	+	M	Mikkel Rasmussen et al 2014

Table S2. Selected differentially expressed genes. Related to Figure 3-5.
Subset of significantly differentially expressed genes detected by comparing patient-derived CHMP2B-mutant cell lines with Cas9-corrected controls. For a full list of significantly DE genes, see Table S3. Genes are grouped based on their association with processes, functions or characteristics of interest for the disease. Lists of genes related to each annotation were retrieved from one of the following sources as indicated: Gene Ontology (GO); WikiPathways; COMPARTMENTS; KEGG: literature (manually curated). For each gene, we report its name, Ensembl identifier, log2 fold change and adjusted P-value. Only significantly differentially expressed genes are reported (adjusted p-value <= 0.05, absolute log2 fold change >=1 and average of normalized read counts >=10). For genes grouped by associated compartment, we also provide the confidence score assigned in COMPARTMENTS; only genes with a confidence score >=3 is shown.

Table S3. Differentially expressed genes. Related to Figure 3-5.
List of significantly differentially expressed genes detected by comparing patient-derived CHMP2B-mutant cell lines with Cas9-corrected controls, and overrepresented terms obtained by comparing differentially expressed genes with expressed genes. For each differentially expressed gene, we report its name, Ensembl identifier, log2 fold change and adjusted P-value. Gene counts normalized by DeSeq2 in the sample are also provided. Only significantly differentially expressed genes are reported (adjusted p-value <= 0.05, absolute log2 fold change >=1 and average of normalized read counts >=10). Overrepresented terms were filtered by excluding redundant annotations (overlap between gene sets >= 50%).

Table S4. **Antibodies used for Immunocytochemistry, Western Blot and Primers used for RT-qPCR. Related to Figure 1-3 and 5.**

Immunocytochemistry				
	Antibody	**Antibody Registry* Identifier**	**Dilution**	**Company**
Astrocyte differentiation	rabbit anti-SOX9	AB_2665492	1:400	CST
	rabbit anti-GFAP	AB_10013382	1:1000	Dako
	rabbit anti-aquaporin4	AB_2274338	1:50	Abcam
	mouse anti-S100β	AB_882426	1:500	Sigma
Reactive Astrocyte	rabbit anti-LCN2	AB_10618739	1:200	Millipore
	mouse anti-TIA1	AB_2201439	1:100	Abcam
	rabbit anti-C3	AB_1240642	1:500	GeneTex
Autophagy pathway	rabbit anti-LC3B rabbit anti-LC3B	AB_881433 AB_881429	1:1000 1:2000	Abcam Abcam
	mouse anti-RAB7	AB_882241	1:1000	Abcam
	guinea pig anti-P62	AB_2687531	1:100	Progen
	mouse anti-LAMP1	AB_2296838	1:400	HB
Secondary antibodies	AF 488 donkey anti-rabbit IgG	AB_2534015	1:1000	TFS
	AF 488 donkey anti-guinea IgG	AB_2535788	1:2000	TFS
	AF 594 donkey anti-rabbit IgG	AB_2556547	1:2000	TFS
	AF 594 donkey anti-goat IgG	AB_2534105	1:1000	TFS
	AF 594 donkey anti-mouse IgG	AB_253578	1:1000	TFS
	AF 647 donkey anti-mouse IgG	AB_162542	1:1000	TFS
Western Blot				
	Antibody	**Antibody Registry* Identifier**	**Dilution**	**Company**
Primary antibodies	*rabbit anti-GAPDH	AB_9485, AB_307275	1:3000 1:3000	Abcam
	*mouse anti-GAPDH	AB_627678	1:4000	SCT
	rabbit anti-LC3B	AB_881429	1:3000	Abcam
	rabbit anti-C3	AB_1240642	1:10000	GeneTex
	mouse- LAMP1	AB_2296838	1:4000	HB
	rabbit-Phospho NF-Kb	AB_10827881	1:1000	CST
	rabbit- NF-Kb	AB_10859369	1:1000	CST
	mouse- Caspase 3	AB_781826	1:500	SCT
Secondary antibodies	IRDye® 800CW Donkey anti-Rabbit IgG (H + L)	AB_621848	1:15,000	LI-COR
	IRDye® 800CW Donkey anti-Mouse IgG (H + L)	AB_621847	1:15,000	LI-COR
	IRDye® 680LT Goat anti-Mouse IgG (H + L)	AB_10706161	1:20,000	LI-COR
	IRDye® 680LT Goat anti-Rabbit IgG (H + L)	AB_10706309	1:20,000	LI-COR
RT-qPCR primers				
Human Primers				
Gene Name	**Forward**	**Reverse**	**Concentration**	**Company**
OPA1	GGCGGAAGACCTCAAGAAAGT	GGCTGGACAAAAGACGTTGAT	10µM	OligoTagc
MFN1	CCAGAAAGTGGTGTGGCACT	GTTTTCACTGCTGACTGCGAG	10µM	OligoTagc
FIS1	GGTGCGGAGCAAGTACAATGA	CGTATTCCTTGAGCCGGTAGT	10µM	OligoTagc

MAP3K9	CTGGAACGGGAGCTCAACAT	TGGTGTCAACTGGATGGCTC	10µM	OligoTagc
DCN	CCCTCCTCCTTTCCACACCT	TTTTCACAACCAGGGAACCTTT	10µM	OligoTagc
GAS6	GACATAGACGAGTGCGCAGA	ACGGCAAGATGTCCTCACAG	10µM	OligoTagc
GAD1	GGGAACTAGCGAGAACGAGG	GGTATCGTACGTTGTGGGGC	10µM	OligoTagc
MT-ND2	TCATAGCAGGCAGTTGAGGC	GGTCGTGGTGCTGGAGTTTA	10µM	OligoTagc
IL17D	GAGTCCCCGGGTCTGGAT	GTGTGGTGGAAGGCACTGAG	10µM	OligoTagc
**GAPDH*	CTCTCTGCTCCTCCTGTTCGAC	TGAGCGATGTGGCTCGGCT	10µM	OligoTagc
Mouse Primers				
Gene Name	**Forward**	**Reverse**	**Concentration**	**Company**
mIl6	GATGCTACCAAACTGGATATAATC	GGTCCTTAGCCACTCCTTCTGTG	10µM	OligoTagc
mc3	ACCCCTTCATTCCTTCCACCT	CCTTACTGGCTGGAATCTTGATGG	10µM	OligoTagc
mLcn2	TCTGTCCCCACCGACCAATG	GGGGAGTGCTGGCCAAATAA	10µM	OligoTagc
mMap3k	ATCAGGAGATGAAGGCCTCAAG	AGGACTGGTTGGGTGAATGC	10µM	OligoTagc
mMfn1	CAGGGACGGAGTGAGTGTCC	GTTTCTGCCATTATGCACCTGGA	10µM	OligoTagc
mFis1	CTGGTGTCTGTGGAGGATCTGA	GAGCCTTTTCATATTCCTTGAGCC	10µM	OligoTagc
mOpa1	CTGCAGGTCCCAAATTGGTT	CTGCAGGTCCCAAATTGGTT	10µM	OligoTagc
MDcn	TTCCTACTCGGCTGTGAGTC	AAGTTGAATGGCAGAACGC	10µM	OligoTagc
mGad1	CCTTCGCCTGCAACCTCCTCGAAC	GCGCAGTTTGCTCCTCCCCGTTCTT	10µM	OligoTagc
mMt-nd2	AGGGATCCCACTGCACATAG	TGAGGGATGGGTTGTAAGGA	10µM	OligoTagc
mIl17d	GGGCGTACAGGATTTCCTAC	AGAGAAGACGGGTGTGCTG	10µM	OligoTagc
mGas6	AAAGGGCCAGAGTGAAGTGA	TTTTCCCGTTTACCTCCAGA	10µM	OligoTagc
*mGapdh	TGCACCACCAACTGCTTAG	GGATGACCTTGCCC	10µM	OligoTagc

AF, Alexa Fluor; TFS, Thermo Fisher Scientific Inc; HB, Hybridoma bank; CST, Cell Signalling Technology; IRDye, Infrared Dye, http://antibodyregistry.org/. GAPDH was used as reference gene, m=mouse.

Supplemental Experimental Procedures

Patient Information

In this study, we have used two unedited FTD3 hiPSC lines carrying CHMP2B mutation (referred to as FTD3 patient 1 and FTD3 patient 2 throughout the study), two corresponding CRISPR/Cas9 gene edited isogenic control hiPSC lines (referred to as Isogenic Control 1, Isogenic Control 2 throughout the study), one heterozygous mutant CHMP2B CRISPR/Cas9 induced hiPSC line (referred to as heterozygous throughout the study), one homozygous mutant CHMP2B CRISPR/Cas9 induced hiPSC line (referred to as homozygous throughout the study) and one corresponding healthy wildtype control hiPSC line (referred to as wildtype throughout the study). The detail information are added to the Table S1. All patients provided written informed consent. The studies were approved by the Ethics Committee of the Capital Region of Denmark (H-4-2011-157) institutional review board.

Generation of Cell Lines

hiPSCs were generated via episomal reprogramming (Addgene, 27077, 27078, 27080) from human dermal fibroblasts obtained from skin biopsies as described in (Zhang et al., 2017). The hiPSC lines were maintained on matrigel (BD Matrigel; 15535739, Stem Cell Technologies) in E8 culture media (05991, Stem Cell Technologies). The media was changed daily, and the cells were passaged every 5-7 days using 0.5 mM EDTA (B52, Thermo Fischer) according to the manufacturer's instructions. All hiPSC lines used in this study were characterized and published earlier in (Rasmussen et al., 2014; Zhang et al., 2017). Karyogram for the CRISPR/Cas9 induced heterozygous and homozygous CHMP2B hiPSC are presented in Figure S5.

CHMP2B Mice

Snap frozen brains of *CHMP2B*$^{wild\text{-}type}$ and *CHMP2B*$^{intron\ 5}$ were kindly provided by Adrian M. Isaacs. The mouse model was published earlier in (Ghazi-Noori et al., 2012). The mouse brain were 6 month-old at the time of study. Mouse brains were dissected and the cerebellum and brainstem were removed. Subsequently, one cerebral hemisphere was used for WB and the other for qPCR.

Neural Induction/ Generation of Neural Progenitor Cells

Neural progenitor cells (NPCs) were generated from each of the hiPSCs by dual SMAD inhibition, using LDN193189, an inhibitor of the BMP pathway (Selleck, S2618) and SB431542, a small molecule inhibitor of the TGFß pathway (Selleck, S1067) (Chambers et al., 2009). The neural differentiation was induced via 3D sphere-based method, according to the previously published method (Chandrasekaran et al., 2017).

Astrocyte Generation

We generated an efficient astrocyte differentiation protocol based on a modified version previously published (Shaltouki et al., 2013). To generate astrocytes, NPCs were first generated via 3D neural induction, where the neuronal rosettes were selected for astrocyte generation. NPCs were then plated at 70% confluence on matrigel in astrocyte differentiation media (ADM) media supplemented with 10 ng/ml of bFGF, 10 ng/ml of Activin A (Thermofisher, PHG9014) & 10 ng/ml Heregulin 1β (HRGβ1) (Peprotech, 100-03), and 200 ng/ml of Insulin Growth Factor-1 (IGF-1) (Peprotech, 100-11) (Shaltouki et al., 2013). Astrocyte maturation was achieved by passaging astrocyte progenitor cells (APCs) few times before plating (at least until passage 5, to switch from neurogenesis to gliogenesis). Enriched astrocyte progenitors were plated at a seeding density of 50.000 cells/cm^2 in astrocyte maturation media (AMM) medium supplemented with 10 ng/ml of Activin A, 10 ng/ml of HRGβ1, 200 ng/ml of IGF1, 1% sodium pyruvate (Thermofischer, 1136070), 2% heat inactivated and toxin free FBS (Invitrogen, 10100147) and 200 µM L-Ascorbic acid 2-phosphate (Sigma, A8960). The medium was changed every other day and cells were differentiated for 35+ days. The efficiency of terminal differentiation astrocytes was monitored for S100β, AQP4, and SOX9 by ICC. In the current study astrocyte progenitor cells were differentiated up to 7 weeks for astrocyte verification; and 10 weeks for the remaining assays: western blot (WB), transmission electron microscopy, cytokine profiling, RNA-seq, qPCR and metabolic assay.

Rapamycin Treatment

To evaluate the rescuing effect of rapamycin on autophagy impairments, cell cultures were treated with rapamycin (R8781, Sigma) before performing the following assays. At 10 weeks of maturation, cell cultures were induced with 200 nM and 500 nM rapamycin in AMM medium to visualize any concentration

dependencies of rapamycin and incubated at 37°C for 24 hours and subsequently fixed for TEM. For ICC, cell cultures were induced with 200 nM and 500 nM of rapamycin at 10 weeks of maturation and incubated for 37°C for 24 hours followed by fixation. Control cell lines were kept in AMM media as reference.

Immunocytochemistry and Confocal Microscopy
Cells were cultured on 0.17 µM glass coverslips coated with matrigel. Cell cultures were fixed in 4% paraformaldehyde (PFA) for 20 min, room temperature (RT), washed 3 times with PBS and permeabilized (0.2% Triton X-100 in PBS; 20 min). After blocking for 30 minutes (at RT in 5% donkey serum) the cells were incubated with primary antibodies (Table S4, ICC panel) overnight at 4°C. On the following day, the isotype specific secondary antibodies (Table S4, ICC panel) were applied (1 hour at RT). Samples were washed in PBS and stained with DAPI (Sigma-Aldrich, D9542) to label the nuclei of the cells. Samples were visualized on a confocal microscope equipped with a Leica TCS SPE microsystem controlled by LAS X software (v 2.0.0.14332).

Puncta Quantification
Puncta (small spherical fluorescence points) were counted by analysing fluorescent images using the Puncta Analyzer plugin of the Image J software. Fifteen different randomly chosen fields from three independent experiments were counted by an independent investigator in a double blinded approach.

MitoTracker ® Assay
Cells for MitoTracker® Red CMXRos (Molecular Probes, M7512) analyses were cultured on 0.17 µM glass coverslips coated with matrigel. Cells were incubated with 100 nM MitoTracker® in DMEM/F-12 medium for 15 min at 37 °C, followed by fixation in 4% PFA in PBS for 15 min, permeabilization in 0.5% Triton X-100 in PBS for 15 min and incubation with DAPI for 7 min at RT. In between each step the samples were washed 3 times in PBS. After the last wash, the glass coverslips were mounted with mounting media and sealed onto slides. Images were acquired by laser scanning confocal microscopy Leica TCS SPE microsystems controlled by LAS X software (v 2.0.0.14332). The analysis was performed on 10 weeks matured astrocyte samples.

Quantitative qPCR
RNA was extracted using RNeasy® Plus Mini Kit (Qiagen, 74134) according to the manufacturer's protocol. cDNA was synthesized from 1 µg of total RNA (from the human samples) in 20 µL reaction using iScript™ cDNA synthesis Kit (BIO-RAD, 1708890). After synthesis, the cDNA was diluted four times with double distilled water and were subjected to PCR amplification with primers (Table S4, primer panel). Likewise for mouse brain samples, 1 µg of CHMP2B mouse brain RNA from three mice per genotype at 6 months of age was synthesized. Quantitative real-time PCR (qPCR) reactions were done in triplicates using the FastStart Lightcycler 480 SYBR Green I Master (Roche, 04707516001) on Lightcycler® 480 real-time PCR system (Roche, Switzerland) for both human and mouse.

RNA-Sequencing Library Preparation
For RNA sequencing, two unedited FTD3 hiPSC lines carrying CHMP2B mutation (FTD3 patient 1, FTD3 patient 2), two corresponding CRISPR/Cas9 gene edited isogenic control hiPSC lines (Control 1, Control 2) and one heterozygous mutant CHMP2B CRISPR/Cas9 induced hiPSC line (heterozygous) were employed for gene expression analysis. The heterozygous astrocytes were used for variant-aware off-target evaluation. The quality of extracted RNA was checked on Agilent 2100 Bioanalyzer system using RNA 6000 nano chip and reagents. All the RNA samples had RIN value > 6. QC passed RNA samples were further used to construct the RNA libraries with TruSeq RNA Library Prep Kit using manufacturer's protocol. The libraries were quantified using Qubit 3.0 and Agilent 2100 Bioanalyzer system using DNA HS chips. qPCR was performed for precise concentration of the libraries and all the libraries were pooled in equimolar concentrations. The pooled libraries were sequenced on Illumina HiSeq 2500 sequencing platform with 1X100 single end reads.

RNA-Sequencing Data Analysis and Functional Association of Differentially Expressed Genes
Transcript reads were pre-processed by trimming low-quality 3' ends and adapter sequences with cutadapt v1.13 (Martin, 2011) (phred quality threshold=30). Reads shorter than 90 nt were removed and all remaining reads were trimmed at the 3' end to a common length of 90 nt. Reads matching rRNAs were extracted with

BBDuk v38.22 (BBDuk) (minimum covered fraction = 0.5, kmer size = 31) based on the annotations available in SILVA v119.1 (Quast et al., 2013). Pre-processed reads were mapped to the human genome (hg38) with HISAT2 v2.1.0 (Kim et al., 2019), resulting in an average of 33,84 M uniquely mapping reads per sample. Alignments were inspected with Samtools v1.9 mpileup function (Li et al., 2009) to confirm the presence/absence of the CHMP2B mutation (Chr3:87,253,711 G>C) and of the silent edits introduced by template-directed Cas9 editing (Chr3:87,253,729 A>C, Chr3:87,253,732 T>G). Non-chimeric reads were assigned to genomic features annotated in GENCODE v29 (Frankish et al., 2019) with feature Counts (Subread v1.6.3) (Liao et al., 2014). Differential expression analysis was carried out with DESeq2 v1.22.2 (Love et al., 2014) by comparing n = 4 patient-derived CHMP2B mutated cell lines (time points 5 and 10 weeks) with their CRISPR/Cas9 gene-corrected isogenic controls. Time point information was introduced in the DESeq2 formula as batch effect. Genes with Benjamin-Hochberg adjusted P-value (Wald test) <= 0.05, absolute log2 fold change >= 1 and mean of normalized counts >= 10 were considered significantly differentially expressed in the comparison between the two groups.
Functional and compartmental labelling was done for the differentially expressed genes by grouping them based on functional or subcellular compartment annotation downloaded from AmiGO v2 (Blake et al., 2015) (GO:0000266, GO:0008053, GO:0000422, GO:0019646, GO:0006119, GO:1900016, GO:1900017, GO:0034351, GO:0034352, GO:0090141), Wikipathways (Slenter et al., 2018) (WP3941, WP408, WP4459, WP534), COMPARTMENTS (Binder et al., 2014) (GO:0005768, GO:0005764, GO:0005739), KEGG (Kanehisa, 2000) (hsa04064, hsa04668), or from manually curated literature [For details refer: Table S2 & S3]. For subcellular compartment annotation, only genes with a confidence cut-off of at least 3 were considered. Additional functional associations between differentially expressed genes with a confidence cut-off of at least 0.8 were retrieved from STRING v11 (Szklarczyk et al., 2019) through the StringApp v1.5 (Doncheva et al., 2019) and further visualized and annotated in Cytoscape v3.7.1 (Shannon et al., 2003). Functional enrichment analysis of differentially expressed genes was computed with the StringApp, setting as background all the genes expressed in our samples (mean of normalized counts >= 10). Results were filtered by excluding annotations showing high redundancy with a more statistically significant annotation (overlap between gene sets >= 50%).

Metabolic Mapping

The culture medium was removed and the cells were washed with PBS (37°C). Cell cultures were subsequently incubated for 90 min at 37ºC in the presence of 2.5 mM [U-^{13}C] glucose or 2.5 mM [1,2-^{13}C] acetate plus 2.5 mM unlabeled glucose (Frandsen et al., 1989). The concentrations of substrates were chosen based on previous studies (Aldana et al., 2017). After the incubation, the medium was collected and the cells were washed with cold PBS (4°C), lysed and extracted with 70% ethanol. The cells were scraped off the dish and centrifuged at 20,000 g for 20 min (4ºC) to separate the soluble extract (supernatant) from the insoluble components (pellet). Cell extracts were lyophilized and reconstituted in water for subsequent biochemical analyses. The cell extracts were separated and metabolites were mapped using a gas chromatograph (Agilent Technologies 7820A chromatograph, J&W GC column HP-5MS, parts no. 19091S-433) coupled to a mass spectrometer (Agilent Technologies, 5977E). The isotopic enrichment was calculated according to (Biemann, 1962). Data are presented as labelling (%) of M+ X, where M is the mass of the unlabeled molecule and X is the number of labelled C-atoms in a given metabolite.

Transmission Electron Microscopy

For transmission electron microscopy (TEM) the cells were fixed at 10 weeks of maturation with 3% glutaraldehyde (Merck, 1042390250) in 0.1 M mNa-phosphate buffer, pH 7.4, post-fixed in 1% osmium tetroxide in 0.1 M Na phosphate buffer, dehydrated stepwise in a graded ethanol series, and embedded in Epon (TAAB, T031). Semi-thin (2 µM) sections were cut with glass knifes on an ultramicrotome (Leica Ultracut, Leica Microsystems, Wetzlar, Germany), stained with 1% toluidine blue O (Millipore, 1159300025) in 1% Borax (LabChem, LC117101). Ultra-thin (50 nm to 70 nm) sections were sectioned with a diamond knife (Jumdi, 2 mm) on an ultramicrotome (Leica Ultracut), contrasted with 2% uranyl acetate (Polyscience, 21447) and lead citrate (Merck, 1073980100), and examined using a Philips CM100 transmission electron microscope operating at 60 kV. Photographs were taken using Olympus Morada 11-megapixel camera and iTEM software (Olympus).

Multiplex Array

Cytokine concentrations were measured in duplicates using the MESO QUICKPLEX SQ 120 imager (MSD) with the software DISCOVERY WORKBENCH 4.0 and the data were normalized to protein content. Only values above detection level and with a CV value below 25 were included.

Real-time assessment of mitochondria respiration function via Seahorse XFe96

Oxygen consumption rate (OCR) was measured using a Seahorse XFe96 Extracellular Flux Analyzer (Agilent, USA). Human APCs from FTD3 patient cell lines and from knock-in cell lines carrying the CHMP2B mutation were seeded in a Seahorse 96-well cell culture microplate at a density of 12,000 cells/well for 10 weeks until they reach astrocytic maturation. On the day of the assay, the cells were washed twice and changed to Seahorse assay medium (unbuffered DMEM (pH 7.4) supplemented with 2.5 mM glucose and 3 mg/L phenol red) and the cells were equilibrated for 10 min at 37°C in a CO2-free incubator. The reagents used to test mitochondrial function were pH adjusted to 7.4. The OCR measurement cycle consisted of 3-min mix and 3-min measurement of the oxygen level. Mitochondrial function assessment was initiated by three baseline OCR measurement cycles. These were followed by the sequential injection of: (a) the inhibitor of ATP synthase, Oligomycin (2 µM final concentration); (b) the uncoupling agent, Carbonyl cyanide 4- (trifluoromethoxy) phenylhydrazone (FCCP, 1 µM); (c) a mixture of the inhibitors of mitochondrial complexes I and III, Rotenone (0.5 µM) and Antimycin A (0.5 µM) with three OCR measurement cycle in between each injection and three final measurement cycles. Oxygen consumption rates were automatically recorded and calculated by the software, Wave (Agilent). Subsequent to the Seahorse analysis, in order to normalize the data, the protein content was measured for each well using the Pierce assay with bovine serum albumin as standard. Results are expressed as mean values ± SEM from 12 wells/plate obtained in triplicate for each condition. Basal respiration was determined by subtracting non-mitochondrial respiration (minimum measurement after rotenone/antimycin injection) from the last measurement obtained before oligomycin injection; maximal respiration, measurement obtained after FCCP injection; for obtaining the oxygen consumption associated to ATP production, the measurement after oligomycin injection was subtracted from the last measurement before oligomycin injection.

CellROX (CellROS)

ROS were detected in cells (5×10^5) stained at 37°C for 30 min with 5 µM (cell lines) CellROX green, according to the manufacture instruction. After staining, the cells were washed and analysed with FACS analyzer.

Co-culture with Astrocyte Condition Media

To assess the effects of neurite outgrowth, condition media obtained from FTD3 related astrocytes and controls were cultured on wild type neurons for 5 days, then cells were fixed using 4% PFA for immunocytochemistry. Wild type neurons were kept in neuronal differentiation media as reference. Neurite length was assessed using neurite tracer software of Image J. The analysis was carried out blinded by an independent investigator.

Western Blot

CHMP2B mouse brain tissues were lysed in tPER™ tissue protein extraction reagent (Thermo Fisher Scientific, 78510) and cell from FTD3 astrocytes and controls were lysed in mPER™ mammalian protein extraction reagent (Thermo Fisher Scientific, 78501) containing protease inhibitor (Complete tablets, Roche Diagnostics 04693116 001) and phosphatase inhibitors (PhosSTOP tablets, Roche Diagnostics 04906845001). 10 µg of protein were separated by NuPAGE™ Novex™ 4-12 % Bis-Tris mini gel (Thermo Fisher Scientific, NP0322BOX) and transferred from gel to membranes by XCell II™ Blot Module (Invitrogen, EI9051). The membranes were incubated with primary antibodies solution overnight at 4°C (refer details and dilutions in supplement table s4, western blot panel). After washing, the membranes were incubated with conjugated secondary antibodies for 1½ hour at RT. All the secondary antibodies are detailed in supplement table S4, western blot panel. Immunoblots were developed with LI-COR Developer Odyssey® FC Imager with 2 minutes at channel 800 and 2 minutes at channel 700 and data was processed using the Image Studio Lite Version 5.2. Expression levels of LC3B, LAMP1, C3, NF-kB and pNF-kB were normalized to GAPDH. In general, we also looked into caspase 3 activity via WB.

Neurite Length Analysis

The cells were plated for neurite outgrowth. At the time of plating, the pre-differentiated neurons (Day 0 of terminal differentiation) appeared spherical in shape with no apparent neurite outgrowth. After 24 hours post-plating, thin neurites began to emerge from the cell bodies of the cells. After 5 days of terminal differentiation in ACM, the neurons were quantified via image analysis as described in (Pool et al., 2008).

Statistical Analysis

For all experiments, data are presented as mean ± standard errors of the mean (SEM) of three independent experiments. Statistical analysis were made in GraphPad Prism 7.03. Statistical analyses were determined using Student's t test or by one way ANOVA with a Tukey's post-test or by two-way ANOVA with Bonferroni post hoc test for differences of mean between each groups. Statistical significance were labelled in figures as (*$p < 0.05$, **$p < 0.01$, ***$p < 0.001$, ****$p < 0.0001$).

Supplemental References

Aldana, B.I., Zhang, Y., Lihme, M.F., Bak, L.K., Nielsen, J.E., Holst, B., Hyttel, P., Freude, K.K., and Waagepetersen, H.S. (2017). Characterization of energy and neurotransmitter metabolism in cortical glutamatergic neurons derived from human induced pluripotent stem cells: A novel approach to study metabolism in human neurons. Neurochem. Int. *106*, 48–61.

BBDuk BBDuk Guide - DOE Joint Genome Institute.

Biemann, K. (1962). The Application of Mass Spectrometry in Organic Chemistry: Determination of the Structure of Natural Products. Angew. Chemie Int. Ed. English *1*, 98–111.

Binder, J.X., Pletscher-Frankild, S., Tsafou, K., Stolte, C., O'Donoghue, S.I., Schneider, R., and Jensen, L.J. (2014). COMPARTMENTS: unification and visualization of protein subcellular localization evidence. Database (Oxford). *2014*, bau012.

Blake, J.A., Christie, K.R., Dolan, M.E., Drabkin, H.J., Hill, D.P., Ni, L., Sitnikov, D., Burgess, S., Buza, T., Gresham, C., et al. (2015). Gene Ontology Consortium: going forward. Nucleic Acids Res. *43*, D1049-56.

Chambers, S.M., Fasano, C.A., Papapetrou, E.P., Tomishima, M., Sadelain, M., and Studer, L. (2009). Highly efficient neural conversion of human ES and iPS cells by dual inhibition of SMAD signaling. Nat. Biotechnol. *27*, 275–280.

Chandrasekaran, A., Avci, H.X., Ochalek, A., Rösingh, L.N., Molnár, K., László, L., Bellák, T., Téglási, A., Pesti, K., Mike, A., et al. (2017). Comparison of 2D and 3D neural induction methods for the generation of neural progenitor cells from human induced pluripotent stem cells. Stem Cell Res. *25*, 139–151.

Doncheva, N.T., Morris, J.H., Gorodkin, J., and Jensen, L.J. (2019). Cytoscape StringApp: Network Analysis and Visualization of Proteomics Data. J. Proteome Res. *18*, 623–632.

Frandsen, A., Drejer, jørgen, and Schousboe, A. (1989). Direct Evidence That Excitotoxicity in Cultured Neurons Is Mediated via N-Methyl-D-Aspartate (NMDA) as well as Non-NMDA Receptors. J. Neurochem. *53*, 297–299.

Frankish, A., Diekhans, M., Ferreira, A.-M., Johnson, R., Jungreis, I., Loveland, J., Mudge, J.M., Sisu, C., Wright, J., Armstrong, J., et al. (2019). GENCODE reference annotation for the human and mouse genomes. Nucleic Acids Res. *47*, D766–D773.

Ghazi-Noori, S., Froud, K.E., Mizielinska, S., Powell, C., Smidak, M., Fernandez De Marco, M., O'Malley, C., Farmer, M., Parkinson, N., Fisher, E.M.C., et al. (2012). Progressive neuronal inclusion formation and axonal degeneration in CHMP2B mutant transgenic mice. Brain *135*, 819–832.

Kanehisa, M. (2000). KEGG: Kyoto Encyclopedia of Genes and Genomes. Nucleic Acids Res. *28*, 27–30.

Kim, D., Paggi, J.M., Park, C., Bennett, C., and Salzberg, S.L. (2019). Graph-based genome alignment and genotyping with HISAT2 and HISAT-genotype. Nat. Biotechnol. *37*, 907–915.

Li, H., Handsaker, B., Wysoker, A., Fennell, T., Ruan, J., Homer, N., Marth, G., Abecasis, G., and Durbin, R. (2009). The Sequence Alignment/Map format and SAMtools. Bioinformatics *25*, 2078–2079.

Liao, Y., Smyth, G.K., and Shi, W. (2014). FeatureCounts: An efficient general purpose program for assigning sequence reads to genomic features. Bioinformatics *30*, 923–930.

Love, M.I., Huber, W., and Anders, S. (2014). Moderated estimation of fold change and dispersion for RNA-seq data with DESeq2. Genome Biol. *15*.

Martin, M. (2011). Cutadapt removes adapter sequences from high-throughput sequencing reads. EMBnet.Journal *17*, 10.

Pool, M., Thiemann, J., Bar-Or, A., and Fournier, A.E. (2008). NeuriteTracer: A novel ImageJ plugin for automated quantification of neurite outgrowth. J. Neurosci. Methods *168*, 134–139.

Quast, C., Pruesse, E., Yilmaz, P., Gerken, J., Schweer, T., Yarza, P., Peplies, J., and Glöckner, F.O. (2013). The SILVA ribosomal RNA gene database project: Improved data processing and web-based tools. Nucleic Acids Res. *41*.

Rasmussen, M.A., Holst, B., Tümer, Z., Johnsen, M.G., Zhou, S., Stummann, T.C., Hyttel, P., and Clausen, C. (2014). Transient p53 Suppression Increases Reprogramming of Human Fibroblasts without Affecting Apoptosis and DNA Damage. Stem Cell Reports *3*, 404–413.

Shaltouki, A., Peng, J., Liu, Q., Rao, M.S., and Zeng, X. (2013). Efficient Generation of Astrocytes from Human Pluripotent Stem Cells in Defined Conditions. Stem Cells *31*, 941–952.

Shannon, P., Markiel, A., Ozier, O., Baliga, N.S., Wang, J.T., Ramage, D., Amin, N., Schwikowski, B., and Ideker, T. (2003). Cytoscape: A software Environment for integrated models of biomolecular interaction networks. Genome Res. *13*, 2498–2504.

Slenter, D.N., Kutmon, M., Hanspers, K., Riutta, A., Windsor, J., Nunes, N., Mélius, J., Cirillo, E., Coort,

S.L., Digles, D., et al. (2018). WikiPathways: a multifaceted pathway database bridging metabolomics to other omics research. Nucleic Acids Res. *46*, D661–D667.
Szklarczyk, D., Gable, A.L., Lyon, D., Junge, A., Wyder, S., Huerta-Cepas, J., Simonovic, M., Doncheva, N.T., Morris, J.H., Bork, P., et al. (2019). STRING v11: Protein-protein association networks with increased coverage, supporting functional discovery in genome-wide experimental datasets. Nucleic Acids Res. *47*, D607–D613.
Zhang, Y., Schmid, B., Nikolaisen, N.K., Rasmussen, M.A., Aldana, B.I., Agger, M., Calloe, K., Stummann, T.C., Larsen, H.M., Nielsen, T.T., et al. (2017). Patient iPSC-Derived Neurons for Disease Modeling of Frontotemporal Dementia with Mutation in CHMP2B. Stem Cell Reports *8*, 648–658.